FINITE ELEMENT MODELING OF THE ORTHOGONAL MACHINING OF PARTICLE REINFORCED ALUMINUM BASED METAL MATRIX COMPOSITES

U. UMER, M. ASHFAQ, J. A. QUDEIRI
H. M. A. HUSSEIN
A. R. AL-AHMARI
FARCAMT, Advanced Manufacturing Institute, King Saud University
Riyadh, Saudi Arabia

e-mail: uumer@ksu.edu.sa

2D finite element models (FEM) are developed to simulate orthogonal machining of particle reinforced aluminum based metal matrix composites (MMC). The models predict cutting forces, chip morphology, temperatures and stresses distributions. The simulations were carried out by developing a fully coupled temperature displacement model. In contrast to the equivalent homogeneous material (EHM) methodology, a heterogeneous model is developed based on reinforcement particle size and volume fraction. This allows models to simulate the local effects such as tool-reinforcement particle interaction, reinforcement particle debonding. The interface between the reinforcement particles and the matrix is modeled by using two approaches; with and without cohesive zone elements. Similarly the chip separation is modeled with and without using a parting line. The effect of different methodologies on the model development, simulation runs and predicted results have been discussed. The results are compared with experimental data and it has been found that the utilization of cohesive zone modeling (CZM) with the parting line approach seems to be the best one for the modeling of MMC machining.

KEYWORDS
finite element models (FEM), metal matrix composites (MMC), cohesive zone modeling (CZM)

1. INTRODUCTION

Metal matrix composites contain at least two separate phases, arranged in a way to obtain properties which cannot be attainable by constituent phases. Most of the MMC have two phases which can be in the form of short or long fibers or in the form of small particles surrounded by a metallic matrix. MMC are gradually replacing conventional metals in many engineering applications due to their superior properties like fracture resistance, higher stiffness and extremely good strength to weight ratio.

MMC are being used in transmission lines, aerospace and automobile parts, various cutting tools specially oil drilling inserts. Some special physical properties make them an attractive choice for superconducting magnets and thermal management applications [Chawla 2006, Davim 2011].

MMC can be subdivided into three broad categories (a) equi-axes particles reinforced (b) short fibers reinforced which may be aligned or not (c) long fibers reinforced. Development of a particular MMC for some specific applications depends on the methods of synthesis and fabrication for stock items. These issues are of particular interest for material technologist and product development engineers [Zhu 2005].

The key issues in processing of MMC are the various problems associated with machining i.e. MMC have poor machinability as compared to conventional metals. This is mainly due to non-homogeneity and abrasive nature of reinforcement particles. Mostly MMC are fabricated with near net shape processes but some machining and finishing cuts are indispensable for final dimensions and surface finishes. Cutting tools such as high speed steel, cast cobalt alloys, cemented carbides and cermets cannot be used for machining of MMC due to high wear rate. Diamond cutting tools are found to be the best option for machining of MMC and they are being utilized in the last ten years for both particles and fibers based MMC [Looney 1992, Schwartz 1997, Muthukrishnan 2008].

Fiber reinforced composites are anisotropic as fibers are not equi-axes, whereas particulate reinforced composites are isotropic like conventional metals. The later provide higher ductility and their isotropic nature make them a better choice as compared to fiber reinforced composites. Machinability of particulate reinforced composites depend on many factors like particulate type, its orientation, tool material, tool geometry and cutting conditions like cutting speed, feed etc.

Numerous studies exist in the literature to analyze machining of MMC using experiments and mostly related to measure performance variables like tool wear, surface roughness, sub surface damage, cutting forces, cutting temperatures and chip morphology [Davim 2011]. It has been found that parameters related to structure of composite greatly affect the machinability. These include reinforcement material, reinforcement type, volume fraction of the particles, base metal properties and overall arrangement of constituent phases. Polycrystalline diamond inserts (PCD) are commonly employed for their machining [Weinert 1993, Quigley 1994]. Use of other ceramics materials like cubic boron nitride (CBN), alumina and silicon nitride are also reported but did not have a major success. Effects of cutting parameters (speed, feed and depth of cut) on machinability of MMC is almost similar to that found in machining of conventional metals with some differences due to abrasive nature of particles. The reinforced particles tend to expelled out from the base metal and slide in front of the cutting tool edge. This results in plowing through the newly generated machined surface and groove marks on it [El-Gallab 1998] [Manna 2003].

A lot of research has been done to model orthogonal machining of MMC. Researchers used three approaches: (a) micromechanics based approach (b) equivalent homogeneous material (EHM) approach (c) Hybrid approach i.e. combination of two [Davim 2011]. The first two approaches have both advantages and disadvantages [Camus 2000]. Debonding of reinforced particle and deformation mechanism can be best modeled by micromechanics approach. However the approach is computationally very expensive as a very fine mesh is required in contrast to conventional modeling. EHM approach is unable to predict local effects such as damage at particle-matrix interface [Arola 1997, Nayak 2005] but it reduces simulation time and can predict some performance variables like cutting forces and temperature with reasonable degree of accuracy. The advantages of both approaches can be obtained using a hybrid approach. A combination of micromechanical and EHM model is developed by Rao et al. [Rao 2007] to study orthogonal cutting. The effects of fiber orientation on the cutting forces, chip formation and fiber damage were analyzed using this approach. EHM was used to model the overall phenomenon while micromechanical model was used near the tool tip and tool-chip interface.

Machining of particulate reinforced MMC has been modeled by various researchers. Except for few, most of the studies are limited to 2D modeling, which can be utilized only for orthogonal machining. Monaghan and Brazil [Monaghan1998] utilized a 2D finite element code FORGE2 to model failure at the particle-matrix interface and the residual stresses while machining Aluminum based MMC. However the interaction between tool and particle was neglected. El-Gallab and Sklad [El-Gallab 2004] developed a model for the machining of SiC reinforced aluminum alloy. It was found that feed has the largest effect on the sub-surface damage and the residual stresses. Both sub-surface damage and residual stresses increase with

increased feed rate. The study was limited to orthogonal machining and the particles were assumed to be perfectly bonded. Other researchers model the tool-reinforcement particle interaction by considering particles on, above and below the tool path [Pramanik 2007, Zhu 2005].

The aim of the present study is to investigate different methodologies to model orthogonal machining of SiC particle reinforced Aluminum based metal matrix composites. The reinforced particle average size is around 20 μm and volume fraction is 20%. A heterogeneous workpiece model based on reinforcement particles size and volume fraction is used to simulate the local effects such as particles debonding and tool-particle interactions. The experimental results published in [Dandekar 2009] have been used to verify the different FE models.

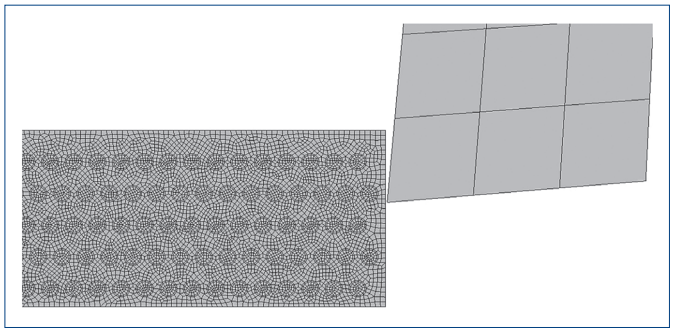

Figure 1. FE model without parting line

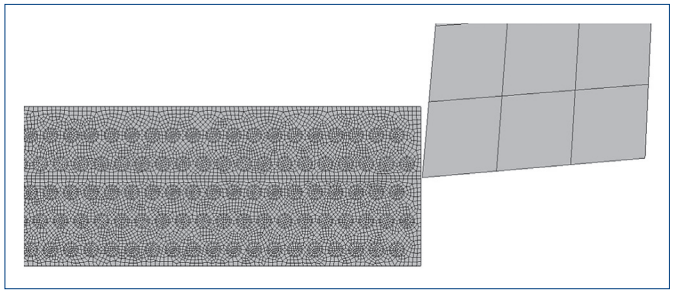

Figure 2. FE model with parting line

	Workpiece (Aluminum Matrix A359 alloy)	Reinforcement particles (SiC)	Cutting tool (PCD)
Density (kg/m^3)	2700	4370	3500
Young 's Modulus (GPa)	72	408	800
Thermal conductivity (W/m/ °C)	180	30	173
Specific heat (J/Kg/°C)	963	706	508

Table 1. Composition and properties workpiece and cutting tool materials

Cutting parameters	
Speed	300 m/min
Feed rate	0.1 mm/rev
Depth of Cut	1 mm
Cutting tool geometry	
Rake angle	5°
Clearance angle	5°
Edge preparation	No

Table 2. Cutting parameters and tool geometry for FE model

2. FINITE ELEMENT MODELS

Finite element (FE) models are developed using a general purpose FE software ABAQUS®. Explicit dynamic analysis with coupled temperature displacement procedure is used for each model. Lagrangian formulation is adopted in which the workpiece is fixed and tool moves with the constant speed. The chip separation is realized by element deletion method using two approaches i.e. with and without a parting line. Similarly the interface between the reinforcement particles and the matrix is modeled by with and without cohesive zone elements. Undeformed meshes for FE models with and without parting line are shown in Fig. 1 and 2. The workpiece and cutting tool materials properties are shown in Tab. 1 and cutting parameters are shown in Tab. 2.

The workpiece and cutting tool materials properties are shown in Tab. 1 and cutting parameters are shown in Tab. 2. For the Aluminum matrix, the Johnson and Cook constitutive model is used to include stress variations due to strain, strain rate, and temperature. This relationship is frequently adopted for dynamic problems with high strain rates and temperature effects.

$$\sigma = (A + B\varepsilon^n)\left(1 + C\ln\left(\frac{\dot{\varepsilon}}{\dot{\varepsilon}_0}\right)\right)\left(1 - \left(\frac{T - T_{room}}{T_{melt} - T_{room}}\right)^m\right) \quad (1)$$

Where is the equivalent plastic strain, the equivalent plastic strain rate, and the operating temperature. The Johnson and Cook equation has five material constants, which are A for yield stress constant, B for strain hardening constant, n for strain hardening exponent, C for strain rate hardening constant, and m for temperature dependency coefficient. T_{room} and T_{melt} are room and melting temperatures and are taken as 20 and 593 °C respectively. is the reference strain rate and it is taken as 1 for the Johnson cook parameters listed in Tab. 3. The material constants are determined from experiment results and can include data over a wide range of strain rates and temperatures. Due to the nonlinear dependence of the flow stress of the material during plastic strain, an accurate value of stress requires expensive iteration for calculation of the increment plastic strain.

JC parameters	A (MPa)	B (MPa)	C	n	m
	255	361	0.01	0.18	5.5

Table 3. The Johnson cook flow model's parameters

The chip separation in the chip is simulated using Johnson and Cook damage law which takes into account strain, strain rate, temperature and pressure [9]. The damage was calculated for each element and is defined by:

$$D = \sum \frac{\Delta\varepsilon}{\Delta\varepsilon_f} \quad (2)$$

Where is the increment of equivalent plastic strain during an integration step, and is the equivalent strain to fracture, under the current conditions. Fracture is then allowed to occur when D= 1.0 and the concerned elements are removed from the computation. The general expression for the fracture strain is given by:

$$\varepsilon_f = (D_1 + D_2\exp(D_3\sigma^*))\left(1 + D_4\ln\left(\frac{\dot{\varepsilon}}{\dot{\varepsilon}_0}\right)\right)\left(1 - D_5\left(\frac{T - T_{room}}{T_{melt} - T_{room}}\right)^m\right) \quad (3)$$

Where $\dot{\varepsilon}_0$ is the reference strain rate and σ^* is the ratio of pressure stress to von-mises stress. D1to D5 arematerial constants and determined by tensile and torsion tests. The Johnson cook damage parameters are listed in Tab. 4.

JC parameters	D_1	D_2	D_3	D_4	D_5
	0.071	1.248	–1.142	0.147	0.1

Table 4. The Johnson cook damage law's parameters

Both the tool and reinforcement materials are modeled as linear elastic without considering fracture.

The interface between the reinforcement particles and the Aluminum matrix is modeled by cohesive zone elements. The Cohesive zone model (CZM) works by defining a relationship between interfacial force (Traction) and crack opening displacement (Separation). The fracture zone is assumed to have initially zero thickness and consists of two identical cohesive surfaces. The separation between the two surfaces under prescribed load is given by a traction-separation law. The stiffness of the cohesive elements degrades as the separation increases and finally the elements are deleted upon a specified maximum value. In this study cohesive elements stiffness and traction-separation behavior is implemented based on study done in [Dandekar 2010].

3. RESULTS

The deformed meshes for the two models A and B are shown in Fig. 2 and 3. Both models are developed without cohesive elements. In model A no parting line is used and shear failure criterion is applied to the whole workpiece. Whereas in model B shear failure is only applied to the parting line.

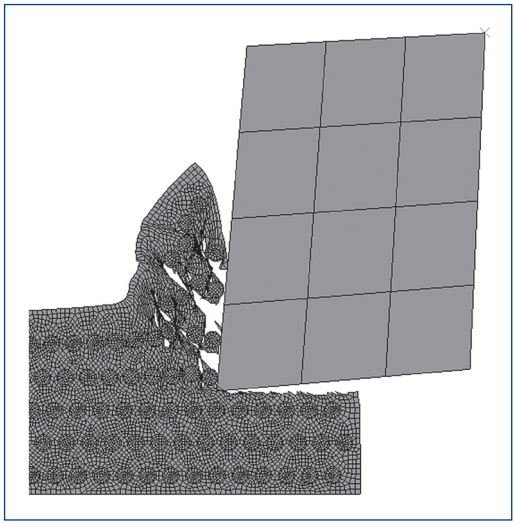

Figure 3. Deformed mesh for model A

It has been observed that both the models are unable to simulate reinforcement debonding at the initial stages due to tool loading. However debonding of reinforcement particles in model A occurred due to material failure around the reinforcement particles and the model is able to simulate tool-particle interaction. In contrast model B simulates a continuous chip with sever material deformation around the reinforcement particles. Experimental studies done by Fathipour et al. [Fathipour 2012] showed serrated chips when machining the same workpiece material at similar conditions.

Models C and D are developed using cohesive elements around the reinforcement particles to simulate debonding at the interface. Shear failure is applied to whole workpiece in both models however model D utilizes a parting line to improve convergence of the model. Also elements are not being deleted in all shear failure models and retain some stiffness throughout the simulation time. Both models are successful in modeling the debonding of the reinforcement particles due to tool loading. Initial deformed meshes for model C are shown in Fig. 5 and 6 simulating the debonding of the reinforcement particle.

Cutting and thrust forces obtained from the experiments and FE model is shown in Figure 7. Both models A and B underestimate forces due to absences of cohesive forces around the reinforcement particles. Cutting forces are lowest for model A due to the application

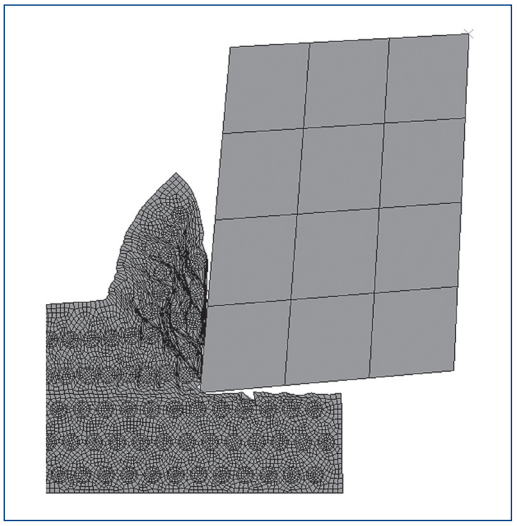

Figure 4. Deformed mesh for model B

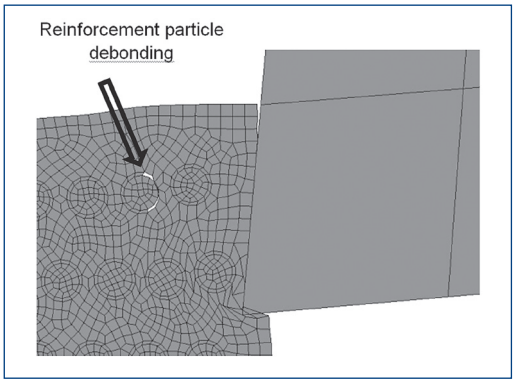

Figure 5. Debonding initiates

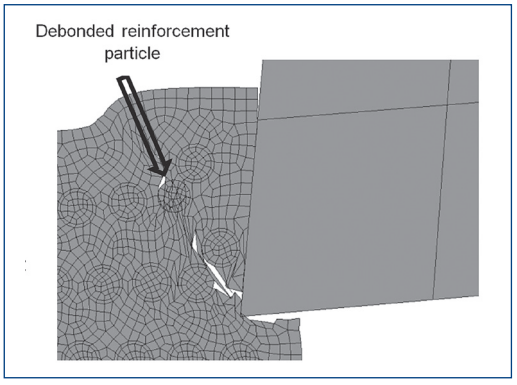

Figure 6. Debonding completed

of shear failure model for the whole workpiece in comparison to model B. Models C and D are predicting higher forces due to the use of cohesive elements and showing minimal differences due to the use of parting line in front of the tool tip. Mises stress for the FE models are shown in Fig. 8 to 11.

The stress distribution pattern for all the models appears to be very same. Due to huge differences in the stress level for reinforcement and matrix the maximum stress is set to 700 MPa to better visualize the stress variation in the workpiece matrix. Mises stresses are lowestfor model A due to shear failure and utilization of no cohesive elements. The chip morphology for all the four models can also be investigated by these figures. The serration on the back of chips can be seen for models with cohesive elements. This is the result of

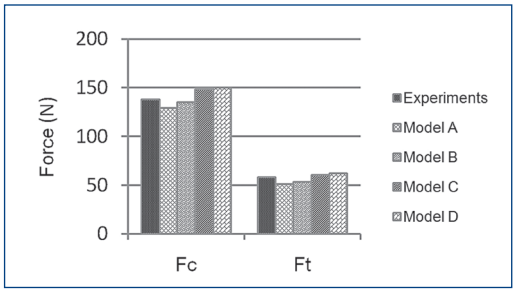

Figure 7. Cutting and thrust forces

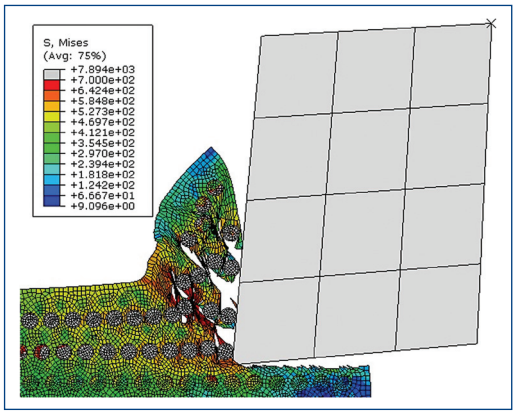

Figure 8. Mises stress for model A

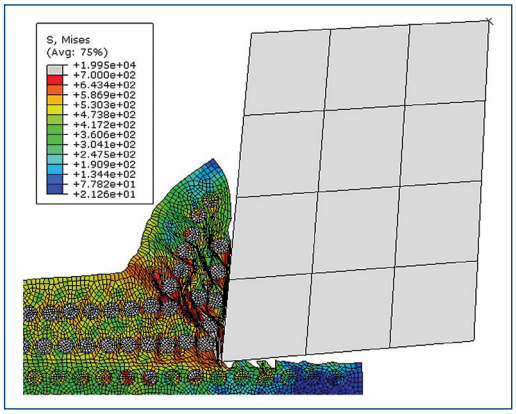

Figure 9. Mises stress for model B

debonding of reinforcement particles and high matrix deformation due to the developing gaps.

Model D performs better with regard to convergence and shows a realistic deformed chip thickness. Also shear localization can also be easily realized for model D. For Model C, the matrix elements along the chip interface are failed and overlaps with chip face. Hence the cohesive models work better with a predefined parting line.

The elements library in ABAQUS® [Abaqus 2012] does not support temperature degree of freedom for cohesive elements. Hence models C and D are unable to predict temperature distributions.

Temperature distributions for models A and B are shown in Fig. 12 and 13. As expected temperatures are lower for model A due to deletion of highly distorted elements. The range of temperaturespredicted by model B is in close agreement with the results obtained by Zhu and Kishawy [Zhu 2005] while machining Alumina based MMC at similar cutting conditions. For both models higher temperatures are predicted corresponding to the region of maximum deformation of the workpiece material around the hard reinforcement particles.

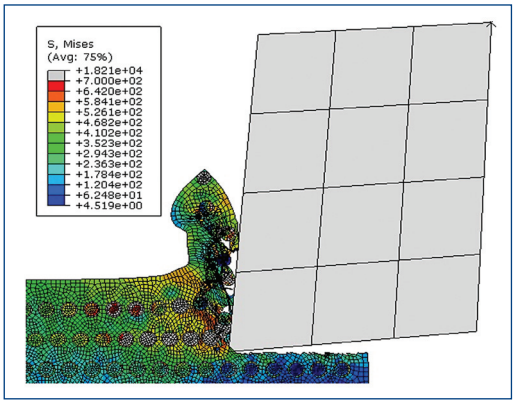

Figure 10. Mises stress for model C

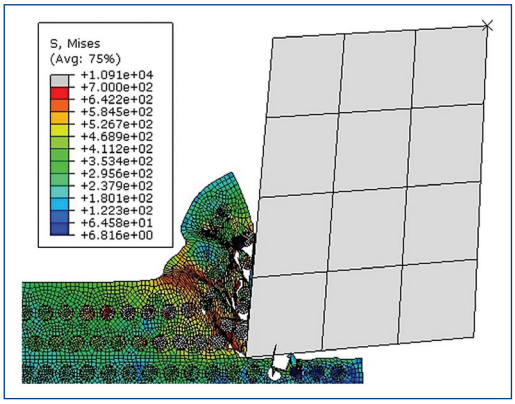

Figure 11. Mises stress for model D

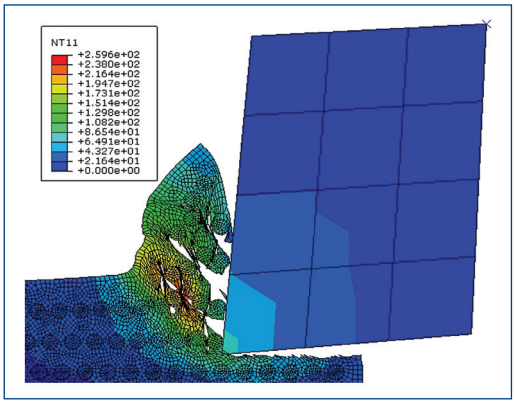

Figure 12. Temperature Contour for model A

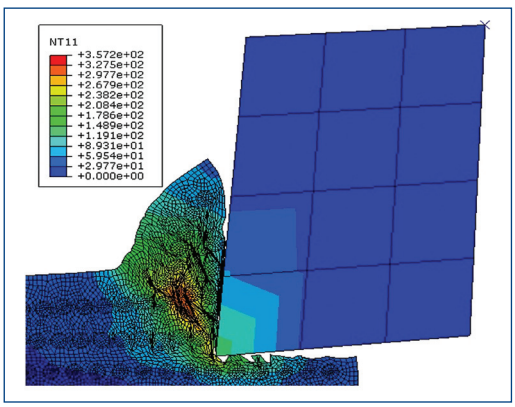

Figure 13. Temperature contour for model B

4. CONCLUSIONS

The developed 2D FE models are successful in predicting the cutting performance variables like chip morphology, cutting forces, temperature and stress distributions.

- Models with cohesive elements interface are able to simulate debonding of the reinforcement particles from the workpiece matrix.
- Models with cohesive elements shows higher cutting forces as compared to non-cohesive models.
- Range of temperatures predicted by FE models in in agreement with the published results and high temperatures are confined to the region of maximum workpiece deformation.
- The FE model based on cohesive elements with pre-defined parting line performs better to simulate serrated chips and shows shear localized regions around the chip face.

ACKNOWLEDGMENTS

We would like to thanks Princess Fatimah Alnijris Research Chair for Advanced Manufacturing Technology (FARCAMT) at Advanced Manufacturing Institute, King Saud University for necessary support for the metal cutting research projects.

REFERENCES

[Abaqus 2012] ABAQUS Documentation. Dassault Systèmes, 2012.

[Arola 1997] Arola, D. , Ramulu, M. Orthogonal cutting of fiber-reinforced composites: a finite element analysis. Int J MechSci, 1997 39 (5), 597–613

[Camus 2000] Camus, G. Modelling of the mechanical behavior and damage processes of fibrous ceramic matrix composites: application to a 2D SiC/SiC. International Journal of Solids and Structures, 2000, 37(6), 919-942

[Chawla 2006] Chawla, N. and Chawla, K. Metal Matrix Composites, 2006

[Dandekar 2009] Dandekar, C. R., Shin, Y. C. Multi-step 3D finite element modeling of subsurface damage in machining particulate reinforced metal matrix composites. Composites Part A: ApplSci Manuf., 2009 40(8), 1231–1239

[Dandekar 2010] Dandekar, C. R. Multi-Scale Modelling and Laser-Assisted Machining of Metal Matrix Composites. Indiana: Purdue University, 2010

[Davim 2011] Davim, J. P. Machining of Metal Matrix Composites, 2011

[El-Gallab 1998] El-Gallab, M., Sklad, M. Machining of Al/SiC particulate metal-matrix composites. Part I: Tool performance. J Mater Process Tech, 1998, 83(1–3), 151–158

[El-Gallab 2004] El-Gallab, M. S. Sklad, M. P. Machining of aluminum/silicon carbide particulate metal matrix composites. Part IV: Residual stresses in the machined workpiece. J Mater Process Tech., 2004, 152(1), 23–34

[Fathipour 2012] Fathipour et al. Investigation of Reinforced Sic Particles Percentage on Machining Force of Metal Matrix Composite. Modern Applied Science, 2012, 6(8), 9-20

[Looney 1992] Looney, L. A. et al. The turning of an Al/SiC metal matrix composites. Journal of Materials Processing Technology, 1992, 33(4), 453-468

[Manna 2003] Manna, A. Bhattacharyya, B. A study on machinability of Al/SiC-MMC. J Mater Process Tech., 2003, 140(1–3), 711–716

[Muthukrishnan 2008] Muthukrishnan, N. et al. An investigation on the Machinability of Al-SiC metal matrix composites using PCD inserts. International Journal of Advanced Manufacturing Technology, Spring Verlag, 2008, 38, 447-454.

[Monaghan 1998] Monaghan, J. Brazil, D. Modelling the flow processes of a particle reinforced metal matrix composite during machining. Composites Part A-Appl S. 1998, 29(1–2), 87–99

[Nayak 2005] Nayak, D. Bhatnagar, N. Mahajan, P. Machining studies of ud-frp composites. Part 2: Finite element analysis. Mach. Sci. Technol. , 2005, 9, 503–528

[Pramanik 2007] Pramanik, A. Zhang, L. C. Arsecularatne, J. A. An FEM investigation into the behviour of metal matrix composites: tool-particle interaction during orthogonal cutting. Int. J Mach Tool Manuf., 2007, 47(10), 1497–1506

[Quigley 1994] Quigley, O. Monaghan, J. O'Reilly, P. Factors affecting the machinability of an Al/SiC metal-matrix composite. J Mater Process Tech, 1994 43(1), 21–36.

[Rao 2007] Rao, G. V. G. Mahajan, P. Bhatnagar, N. () Machining of UD-GFRP composites chip formation mechanism. Compos Sci Technol. , 2007, 67 (11–12), 2271–2281.

[Schwartz 1997] Schwartz, M. M. Composite Materials Fabrication. Processing and applications, 1997

[Weinert 1993] Weinert, K. König, W. A consideration of tool wear mechanism when machining Metal Matrix Composites (MMC). Ann CIRP, 1993, 42 (1), 95–98

[Zhu 2005] Zhu, Y. and Kishawy, H. Influence of Alumina particles on machining of MMC. International Journal of Machine tool and manufacture, 2005, 389-398

CONTACT:

Usama Umer, Assistant Professor
FARCAMT Advanced Manufacturing Institute
King Saud University, College of Engineering
Riyadh 11421, P. O. Box: 8000, Saudi Arabia
tel.: +996 114 699 712, e-mail: uumer@ksu.edu.sa

Mohammad Ashfaq, Assistant Professor
FARCAMT, Advanced Manufacturing Institute,
P. O. Box: 8000, King Saud University
Riyadh 11421, Saudi Arabia
tel.: +966 114 697 372, e-mail: mashfaq@ksu.edu.sa

Jaber Abu Qudeiri, Assistant Professor
FARCAMT, Advanced Manufacturing Institute,
P. O. Box: 8000, King Saud University
Riyadh 11421, Saudi Arabia
tel.: +966 114 699 711, e-mail. jqudeiri@ksu.edu.sa

Hussein Mohammed Abdalmonaem Hussein, Assistant Professor
FARCAMT, Advanced Manufacturing Institute,
P. O. Box: 8000, King Saud University
Riyadh 11421, Saudi Arabia
tel.: +966 116 709 68, e-mail: hhussein@ksu.edu.sa

Prof. Abdul Rahman Al-Ahmari
FARCAMT, Advanced Manufacturing Institute,
P. O. Box: 8000, King Saud University
Riyadh 11421, Saudi Arabia
tel.: +966 114 676 664, e-mail: alahmari@ksu.edu.sa